JOURNAL OF GEOPHYSICAL RESEARCH: PLANETS, VOL. 118, 179–189, doi:10.1029/2012JE004225, 2013

Searching at the right time of day: Evidence for aqueous minerals in Columbus crater with TES and THEMIS data

Alice M. Baldridge,[1] Melissa D. Lane,[1] and Christopher S. Edwards[2]

Received 3 August 2012; revised 8 November 2012; accepted 14 November 2012; published 12 February 2013.

[1] The primary objective of the Thermal Emission Imaging System (THEMIS) experiment, which has been in orbit at Mars since early 2002, is to identify minerals associated with hydrothermal and subaqueous environments. Data from THEMIS have supported the presence of clays, silica-rich deposits, and chlorides but has not before provided definitive evidence for the presence of sulfates. This is an especially puzzling result given that sulfates have been extensively identified with other instruments at Mars. If present, sufficiently exposed, and in high enough abundances, such minerals should be detectable in orbital thermal infrared spectra at the resolution of THEMIS. The extended mission proposal for THEMIS on Mars Odyssey suggests that the detection of all minerals may be enhanced by observing at an earlier time of day and thus at warmer temperatures. Therefore, in 2009, Odyssey moved to an earlier orbit time. Here, we examine THEMIS data collected when the earlier orbit time coincided with the Martian local (southern) late summer (Ls = 270) for Columbus crater where Compact Reconnaissance Imaging Spectrometer for Mars (CRISM) data have detected a number of aqueous minerals. Some of the warmest THEMIS images show evidence for aqueous minerals, although not in the same locations where CRISM finds the highest concentrations. Several factors contribute to this result, including differences in the diurnal temperature curve and levels of induration and particle size. For THEMIS, earlier time-of-day and proper seasonal observations combine to provide warm surface temperatures and ideal low atmospheric opacity that significantly increases the ability to definitively identify low spectral contrast aqueous minerals at the surface of Mars.

Citation: Baldridge, A. M., M. D. Lane, and C. S. Edwards (2013), Searching at the right time of day: Evidence for aqueous minerals in Columbus crater with TES and THEMIS data, *J. Geophys. Res. Planets*, *118*, 179–189, doi:10.1029/2012JE004225.

1. Introduction

[2] The Thermal Emission Imaging System (THEMIS) has been in orbit at Mars since early 2002 [*Christensen et al*., 2004]. The primary objective of the THEMIS experiment is to identify minerals associated with hydrothermal and subaqueous environments including carbonates, clay, chlorides, silica, and sulfates. Of these, data from THEMIS have thus far supported the presence of clays [*Michalski et al*., 2006], silica-rich deposits [*Bandfield*, 2008], and chlorides [*Osterloo et al*., 2009] but has not before provided definitive evidence for the presence of sulfates. Given the extensive morphologic evidence for aqueous processes on the surface of Mars and the long-standing assumption that sulfates should be a dominant alteration product at the Martian surface [*Clark and Van Hart*, 1981; *Burns*, 1987], this null result is unexpected because the THEMIS instrument is sensitive to the wavelength region where sulfates exhibit a strong emissivity absorption feature [*Farmer*, 1974; *Lane*, 2007]. It is especially puzzling because of the detection of sulfates over broad regions of Mars in the visible near-infrared (VNIR) by the Mars Express Observatoire pour la Minéralogie, l'Eau, les Glaces et l'Activité (OMEGA) and the Compact Reconnaissance Imaging Spectrometer for Mars (CRISM) [*Gendrin et al*., 2005; *Langevin et al*., 2005; *Swayze et al*., 2008; *Lichtenberg et al*., 2009; *Wray et al*., 2011] and surface detections by the Miniature Thermal Emission Spectrometer (mini-TES) [*Glotch et al*., 2006; *Lane et al*., 2008] and Mossbauer Spectrometer [*Klingelhofer et al*., 2004].

[3] *Stockstill et al*. [2007] specifically targeted deposits in Martian paleobasins with THEMIS to search for such evaporite deposits (a common formational environment for sulfates). If still present, sufficiently exposed, and in high enough abundances (e.g., >10–15%), evaporites should be detectable in orbital thermal infrared (IR) spectra at the resolution of THEMIS [*Baldridge and Christensen*, 2004]. However, *Stockstill et al*. [2007] found no evidence for evaporites and concluded that evaporite minerals may be present but below the detection limits for THEMIS or are buried by dust or

[1]Planetary Science Institute, Tucson, Arizona, USA.
[2]Division of Geological and Planetary Sciences, California Institute of Technology, Pasadena, California, USA.

Corresponding author: A. M. Baldridge, Planetary Science Institute, 1700 East Fort Lowell, Suite 106, Tucson, AZ 85719, USA. (abaldridge@psi.edu)

2169-9097/13/2012JE004225

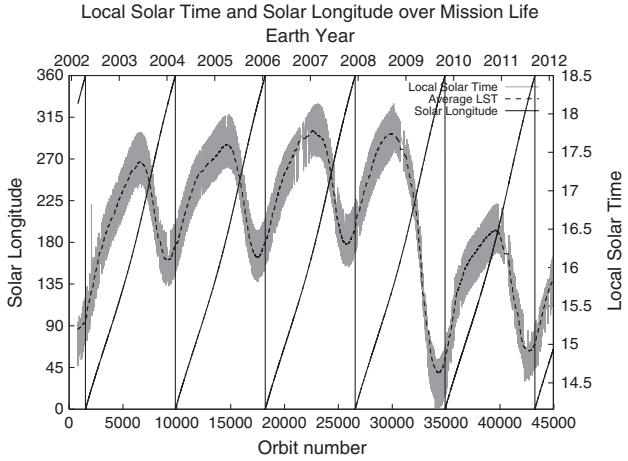

Figure 1. Odyssey LTST (gray), LMST (dashed), and solar longitude over the life of the mission. LTST oscillates approximately ±40 minutes around LMST. Although THEMIS obtains optimal imaging near 15:00, Mars Odyssey LMST was set at approximately 17:15 for the first 7 years of the mission to accommodate the Gamma Ray Spectrometer. The plot shows the LMST oscillating between 16:30 and 18:00 between Ls = 270 and Ls = 150 during the initial phase and the first and second extended missions. In the third extended mission, the orbit was adjusted to a 15:45 LMST to optimize data collection with warmer surface temperature. With this change, the orbit time oscillates between approximately 15:00 and 16:30 corresponding to Ls ~ 300 and Ls ~ 180.

other rocks. Additionally, *Stockstill et al*. [2007] noted that improvements to the THEMIS signal-to-noise ratio (SNR) would be achieved by acquiring additional data at earlier local times (late afternoon as opposed to early evening) and examining this warmer data might permit the detection of evaporite minerals. Indeed, the extended mission proposal for THEMIS on Mars Odyssey suggests that the detection of all minerals may be enhanced by observing at an earlier time of day and thus at warmer temperatures [*Christensen*, 2011].

[4] Mars Odyssey is in a near-polar Sun-synchronous orbit [*Christensen et al*., 2004]. To obtain high-quality daytime IR measurements required for robust compositional analysis, the THEMIS instrument should be operated at local true solar times (LTST) earlier than 17:00 and would achieve the best imaging nearer to 15:00. However, to keep the Sun out of the Gamma Ray Spectrometer cooler field of view (an instrument sharing the Mars Odyssey spacecraft platform), a minimum LTST of 16:00 was required and earlier times could not be accommodated. During the first approximately 3000 orbits, as Odyssey was drifting toward a regular orbit, THEMIS was operating between 15:00 and 16:00, allowing observations of warm surface temperatures (Figure 1). However, during the primary and the first two extended phases of the mission, the Mars Odyssey LTST oscillated approximately ±40 minutes around 17:15 [local mean solar time (LMST)] as a compromise between the constraints of the two instruments. Average surface temperatures at the equator during this oscillation can vary by as much as 20° [*Spanovich et al*., 2006], with typical values around 220 to 260 K. Optimal observing conditions for IR mineral mapping occur during mission phases when the LTST is earliest in the afternoon and when the atmosphere has the lowest dust and water ice opacity. To enhance surface observations, the THEMIS team proposed in the third extended mission proposal that the orbit be moved to a 15:45 PM LMST orbit to optimize data collection with warmer surface temperatures. The maneuver that brought Odyssey to this earlier LMST orbit began in early 2009 and allowed for a period during the summer of 2009 with LMST of approximately 15:00 (Figure 1).

[5] Here we examine one example of a proposed paleolake [*Wray et al*., 2009] on Mars for which examination of VNIR data has detected a number of aqueous minerals [*Wray et al*., 2011]. Additionally, THEMIS data thereof were collected when the earlier orbit time coincided with the Martian local (southern) late summer (Ls = 270). During this time of year, observations at some of the warmest surface temperatures are enhanced by improved atmospheric clarity (minimal dust storm activity).

2. Background

[6] Columbus crater in the Terra Sirenum region of the ancient Martian cratered southern highlands has been investigated using CRISM data and was found to contain light-toned layered deposits with interbedded sulfate and phyllosilicate minerals [*Wray et al*., 2009, 2011]. Hypotheses for the origin of the Columbus crater deposits include groundwater cementation of crater-filling sediments and/or direct precipitation from subaerial springs or in a deep (~900 m) paleolake [*Wray et al*., 2011]. Hydrated sulfate deposits form a discrete ring around the walls of Columbus crater (seen as the band of red or higher thermal inertia material in Figure 2), and on the crater floor, aqueous mineral deposits are exposed beneath younger materials, possibly lava flows [*Wray et al*., 2009, 2011]. A variety of minerals were identified using CRISM data in the crater including gypsum, polyhydrated and monohydrated Mg/Fe-sulfates, and kaolinite in addition to smaller deposits consistent with smectites and jarosite. Additionally, chloride deposits were detected in the surrounding plains of Terra Sirenum [*Osterloo et al*., 2007]. Although the surrounding chloride and Columbus crater sulfate deposits may not be directly related, they both provide strong evidence for the diversity and extent of aqueous deposition/alteration in this region.

3. Methods

[7] THEMIS is equipped with an IR focal plane and an uncooled 320 × 240 pixel detector. The IR imager has nine spectral channels centered at wavelengths between 6.3 and 15.3 μm with a Martian-surface spectral sampling of 100 m per pixel [*Christensen et al*., 2004]. *Christensen et al*. [2004] and *Bandfield et al*. [2004] present detailed descriptions of the calibration and uncertainties associated with the data. The THEMIS data used in this study are listed in Table 1 and the image locations are shown in Figure 3.

[8] A THEMIS daytime IR band 9, a proxy for temperature, mosaic was used to determine morphology. In these images, temperature accentuates shadows and slopes, making these data ideal for analyzing topography. Combined with colorized thermal inertia maps derived from THEMIS

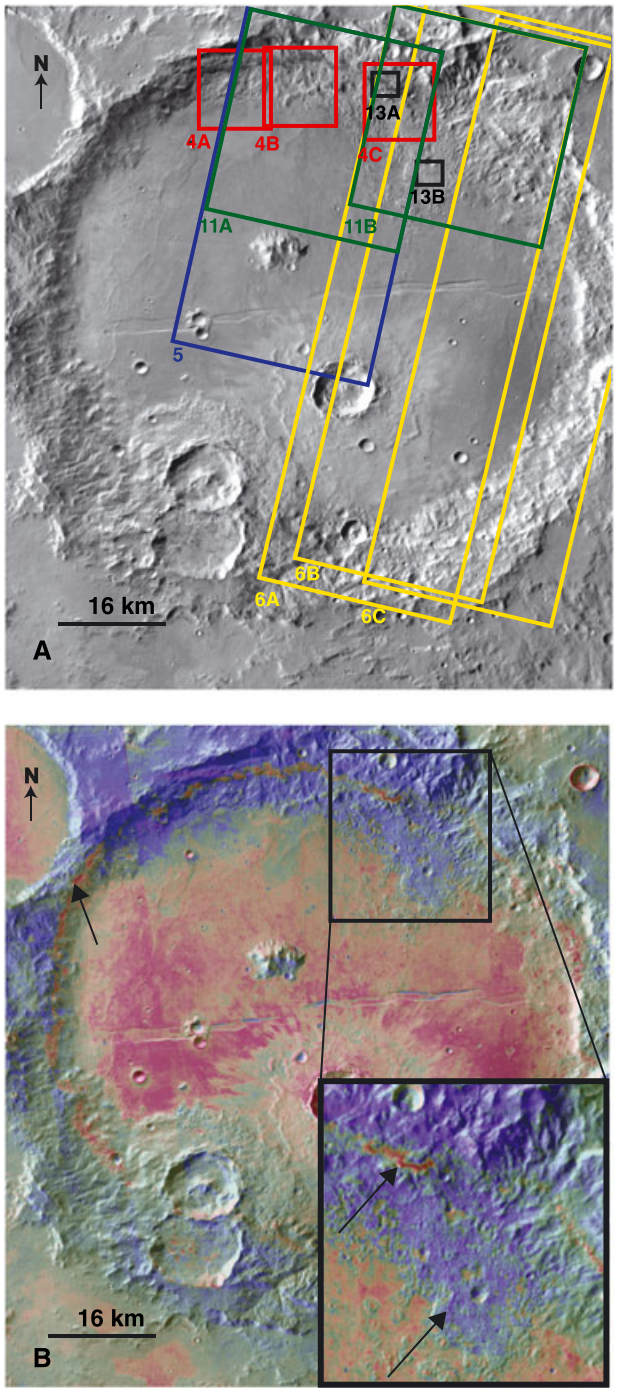

Figure 2. (A) Columbus crater (29°S, 166°W) THEMIS daytime IR band 9 mosaic. Here and subsequently, numbered outlines indicate locations of future figures. (B) THEMIS daytime IR band 9 mosaic to show topography, colorized with THEMIS nighttime temperature to approximate thermal inertia. Blue regions are cold at night and therefore interpreted to have low thermal inertia. Red regions are warm at night and are interpreted as having high thermal inertia. The higher thermal inertia ring midway up the crater wall is found to contain sulfates and phyllosilicates as evidenced in CRISM data. (inset) Arrows point to the regions of the wall-ring unit and the wall-base unit that will be discussed throughout this article and shown in more detail in subsequent figures.

band 9 nighttime temperature data, these data are invaluable for correlating high thermal inertia units (bedrock or cemented units) with composition and providing geographic context.

[9] THEMIS images were identified using Java Mission-Planning and Analysis for Remote Sensing (JMARS; jmars.asu.edu), a data visualization and geographic information system software developed to provide analysis tools for application to data from various Mars orbiters [*Weiss-Malik et al*., 2005]. Stacked display of multiple images in JMARS allowed correlation and comparison of units over multiple orbits and throughout the region of interest. In addition, JMARS allowed images available over the region of interest to be sorted by orbit, Mars' season, and average surface temperature. The THEMIS data used in this study include both warm (240–290 K) and cool (<240 K) average surface temperatures collected over the lifetime of the mission (up to the beginning of 2010). The increase in surface temperature translates into an increase in SNR and should increase the ability to identify previously challenging mineralogy. As shown in this article, the most direct cause of increase in SNR is the measured surface temperature and not an instrument effect.

[10] Decorrelation stretched (DCS) radiance images [*Gillespie et al*., 1986] were used as the primary means for detecting and differentiating unique spectral units and therefore surface compositions. This technique is especially useful for THEMIS IR data because compositional differences are often represented as subtle differences between bands. The purpose of a DCS is to maximize the spectral difference between different bands of data. As such, the data are stretched along second-order variability (spectral features) and not overall temperature (overall brightness, which is highly correlated between spectral bands). A DCS of THEMIS radiance bands 9, 6, and 4 (as mapped to red, green, and blue, respectively) is useful for detecting sulfates and high silica units and distinguishing them from surface type 1. All of these compositions have spectral minima in bands 5 and 4 (near the 9 μm wavelength), but silica and sulfate compositions have significantly higher values in bands 9 and 6. Therefore, in a band 9-6-4 DCS image, these units appear yellow (low in blue or high in both red and green) and surface type 1 compositions are pink (high in red and blue or low in green).

[11] The THEMIS emissivity images and spectra used in this study were individually corrected for atmospheric contributions using the methods described by *Bandfield* [2004]. This method uses atmospherically corrected regional Thermal Emission Spectrometer (TES) spectra as tie-points for constant radiance offset correction and finally for surface emissivity retrieval. Average spectra from at least 50 pixels of contiguous unique spectral units were collected from the THEMIS emissivity data and compared with similar units from different THEMIS images within the basin and with the library database of laboratory-derived mineral emissivity spectra [*Christensen et al*., 2000] degraded to THEMIS spectral resolution.

[12] Additionally, mineral concentration maps were created for the atmospherically corrected emissivity data by performing a linear least squares fit of end-members to THEMIS pixels [*Ramsey and Christensen*, 1998]. The concentrations and root-mean-square (RMS) error between measured and modeled spectra are used to estimate abundance of a given mineral and the quality of the spectral model. End-

Table 1. THEMIS IR Image Data Used in This Study

Image ID	Solar Longitude (Ls)	Earth Date	Mission Phase	LMST	Average Surface Temperature	Maximum Surface Temperature	Minimum Surface Temperature
I07746002	259.708	9/13/2003	Primary	16.789	263.66	294.47	227.51
I09718002	***353.868***	***2/22/2004***	***Primary***	***16.109***	***226.80***	***258.40***	***179.22***
I10030004	***6.680***	***3/19/2004***	***E1***	***16.217***	***233.79***	***264.30***	***197.70***
I18329003	***4.862***	***1/31/2006***	***E1***	***16.262***	***238.87***	***267.18***	***206.32***
I33103002	276.633	5/31/2009	E3	15.316	288.53	307.11	266.32
I33914002	316.753	8/6/2009	E3	14.657	285.94	304.43	258.51
I34488006	342.753	9/23/2009	E3	14.605	268.53	288.70	240.61
I34800002	356.024	10/18/2009	E3	14.709	262.40	286.26	230.61
I34825003	357.063	10/20/2009	E3	14.708	263.41	285.37	234.48
I35137002	9.750	11/15/2009	E3	14.891	253.43	279.14	212.66
I35499002	23.897	12/15/2009	E3	15.166	244.10	275.98	201.32
I35811002	35.692	1/9/2010	E3	15.415	235.17	267.50	189.92
I35811002	35.692	1/9/2010	E3	15.415	235.17	267.50	189.92

member spectra were chosen from higher spectral resolution TES spectral shapes (e.g., surface types 1 and 2 spectral shapes [*Bandfield et al*., 2000b]) and from laboratory-derived mineral libraries [*Christensen et al*., 2000; *Michalski et al*., 2006; *Lane*, 2007; *Baldridge*, 2008]. At 14.88 μm (band 10), the atmosphere of Mars is opaque, so THEMIS cannot see the surface of the planet. THEMIS bands 1/2 values were measured relative to an assumed scene-averaged emissivity of 1 for the atmospheric correction and are therefore only used in a relative sense. Therefore, only bands 3 to 9 of each pixel were unmixed [*Bandfield et al*., 2004] using THEMIS resolution degraded spectra of (1) regional TES spectrum (similar to surface type 2), (2) spectrum representing a mixture of Mg and Ca sulfate, (3) average Mg/Fe clay spectrum, (4) water ice cloud spectral shape [*Bandfield et al*., 2000a], and (5) a blackbody spectrum [*Bandfield et al*., 2004]. Average RMS errors between measured and modeled spectra are anticorrelated with surface temperature and are primarily due to random noise. This relationship indicates that no additional spectral end-members are necessary to model the data.

[13] When regions of interest were large enough to be covered by more than two to three TES pixels, spectra were extracted and averaged. Average TES spectra were atmospherically corrected using the methods of *Bandfield et al*. [2000b] and unmixed using a spectral end-member library similar to *Rogers and Christensen* [2007] that included several sulfate mineral spectra [*Lane*, 2007; *Baldridge*, 2008] using the methods of *Bandfield et al*. [2000b].

[14] In 2009, when Odyssey reached its new earlier orbit time, Columbus crater was specifically targeted to acquire data with improved SNR and enhance the probability of the detection of aqueous mineralogy identified by CRISM. Complete coverage of Columbus crater was achieved between August 2009 and November 2009 when the LMST was between 14:30 and 15:00. During this time, the average surface temperature was 270 K compared with 253 K for all previous late summer images observed at Columbus crater (Table 1). The warmest of these images was observed in May 2009 (I33103002) and August 2009 (I33914002), with average surface temperatures above 280 K. These warmest images have saturated pixels that correspond to Sun-facing slopes. Occasionally, images with very warm areas (e.g., sunlit slopes in an early orbit) can exceed the commanded dynamic range of the THEMIS IR instrument. The dynamic range is set by a predicted gain and offset once per image in the acquisition command sequence. This gain and offset control the conversion of the digital 12-bit data (0–4096) to 8-bit data (0–255) for down-linking to Earth. This gain and offset conversion is applied to reduce the overall data volume sent to Earth and increase the number of images that can be stored on the spacecraft solid-state memory. If the

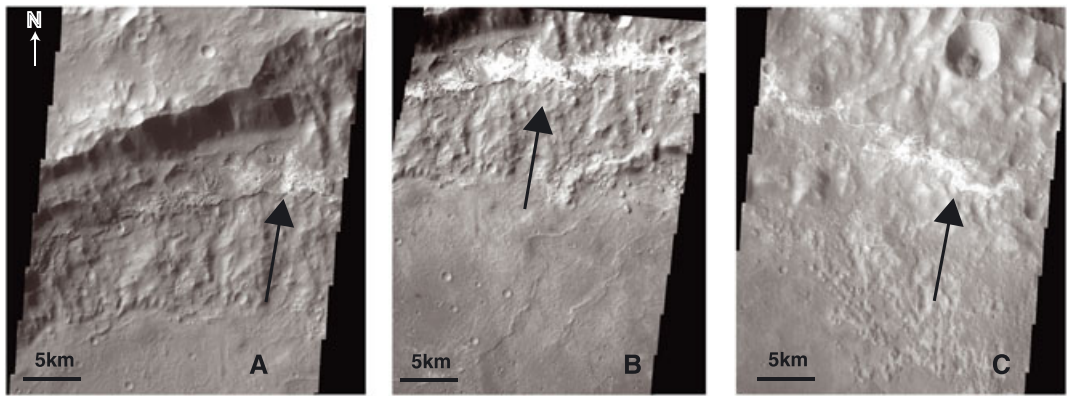

Figure 3. THEMIS visible images (band 3) of the northern wall ring in Columbus crater from THEMIS V02528003, V15571005, and V3516205. The ring consists of light-toned materials.

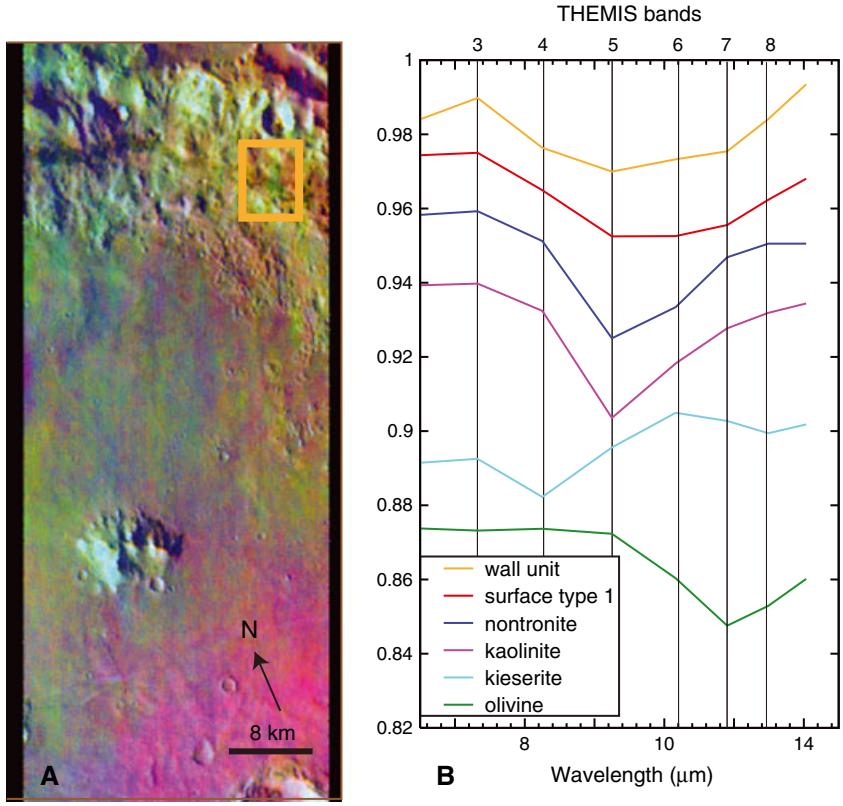

Figure 4. (A) DCS THEMIS radiance image I07746002. Bands 9, 6, and 4 were projected as red, green, and blue, respectively. The wall unit appears yellow in this stretch, indicating lower band 4 values consistent with surfaces that contain phyllosilicates and sulfates. (B) Spectra were carefully selected from the emissivity along the wall unit within the yellow box. Comparison of the average spectrum extracted from this region with surface type 1 and possible end-member spectra. The wall unit spectrum closely resembles surface type 1 with slightly lower values in band 4 but do not qualitatively indicate the presence of sulfates or phyllosilicates. Spectra are offset for clarity.

gain and offset are set too low by mission planners, data loss occurs when the data variation in the 12-bit number cannot be adequately represented in the 8-bit data. Any saturated data will be set to 255. Undersaturated data may also play an equally important role in cold data, where data clipping occurs on the low end of the 8-bit data range rather than on the high end. Images with oversaturated or undersaturated pixels were excluded from analysis because destriping, deplaiding, and other THEMIS cleanup algorithms [*Edwards et al*., 2011] used on images with these oversaturated/undersaturated pixels can introduce errors to neighboring data and make the calibration quality of the overall image uncertain. When the image cleanup algorithms are applied over the saturated pixels, they can introduce spectral errors because the saturated pixels artificially raise or lower the values of surrounding pixels in one or more bands and the result could be confused with physical spectral variability. There are additional cleanup/calibration algorithms that are applied before masking operations suggested are undertaken (e.g., destripe, deghost, uddw, and rtilt; see davinci.asu.edu for a description of these routines) and the suggested parameters do not exist for these early calibration routines. Due to the inherently difficult nature of detecting sulfates with THEMIS, we have elected to not investigate any data with saturated data to avoid any potential complications that could lead to false positives or effects that cannot be easily characterized.

[15] THEMIS images I34488006 and I34800002 are the warmest images that do not contain saturated pixels (Table 1), cover portions of the area covered by I07746002, and were chosen for comparison with previous data. It should be noted that these three images have average surface temperatures in the range of 260 K across the scene, although the two newer images were observed in the late southern summer at approximately 14:45 and the previous image was observed in the early southern summer at almost 17:00. Temperature curves for the planet indicate that the Southern Hemisphere is warmer at Ls = 260 than at Ls = 350, but the earlier time-of-day observations in the late summer has comparable warm temperatures. In addition, three images were chosen covering this region of the crater to illustrate the some of the coldest surface temperatures (bold italic in Table 1).

4. Results

[16] Initially, regions of interest were identified using a colorized nighttime radiance data mosaic overlain on daytime radiance for morphology (Figure 2). In this mosaic, a ring of warmer material was identified in the crater wall.

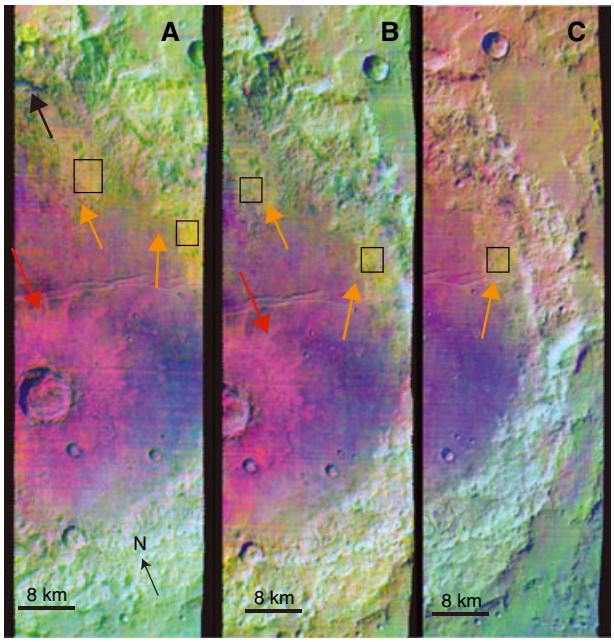

Figure 5. DCS THEMIS radiance images I34488006 (A), I34800002 (B), and I35137002 (C). Bands 9, 6, and 4 were projected as red, green, and blue, respectively. The small crater ejecta are more pronounced in these images than in earlier mission data (red arrows). The crater wall and deposits at the base of the wall also appear more distinct (yellow arrows). The wall ring, however, appears dark in (A; black arrow), indicating that it is colder than the surrounding materials. (black squares) Regions where spectra were collected and averaged (Figure 6). The box in the upper left region of (A) is also where TES spectra were averaged (Figure 7).

The ring is warm (bright) in nighttime images and cool (dark) in daytime images, indicating that it is composed of rocky or indurated materials [*Mellon et al*., 2000; *Ruff and Christensen*, 2002; *Christensen et al*., 2003]. This unit is composed of light-toned deposits (Figure 3) that trace nearly continuously around the eastern, northern, and western crater walls at a near-constant elevation [*Wray et al*., 2011]. Using CRISM data, Wray et al. identified the composition of the wall-ring material as containing both gypsum ($CaSO_4 \cdot 2H_2O$) and Mg/Fe sulfates of nonspecific mineralogy. In addition, outcrops exposed at the base of the northeast crater walls contain mixtures of polyhydrated sulfates, Al-phyllosilicates, and possible alunite [*Wray et al*., 2011]. To support the *Wray et al*. [2011] study, the warmest THEMIS image available (I07746002; see Table 1) that covered the wall unit was processed as described above (Figure 4a). In the publication of *Wray et al*. [2011], this image was the only one that covered the crater in which the wall unit stood out as a somewhat distinct spectral unit. Additionally, distinct units were not identified in THEMIS images of other units in the crater that *Wray et al*. [2011] identified as being sulfate-bearing. In the 9-6-4 DCS image of I07746002, the wall ring and associated floor units appear slightly more yellow than the surrounding terrain, indicating a lower relative band 4 value. Spectra from these regions are consistent with the presence of sulfates or a high silica phase, but the presence of sulfates is not "required" to fit the spectral shapes (Figures 4b and Figure 6).

[17] The DCS images of I34488006 and I34800002 display several more distinct spectral regions (Figure 5). The impact crater ejecta and the central crater appear purple in a 9-6-4 image characteristic of an olivine-rich basalt [*Christensen et al*., 2003; *Hamilton and Christensen*, 2005; *Rogers et al*., 2005, 2009; *Edwards et al*., 2008; *Bandfield et al*., 2011]. The crater wall and the outcrops at the base of northeast and eastern walls have a yellow tone, indicating a relatively low surface emissivity in band 4. Both the ejecta and the wall units appear more distinct in these images than in the previous image as judged by the better definition of the crater ejecta and the contrast of the wall units with the surrounding terrain. The wall ring appears dark in newer data, indicating a relatively low kinetic surface temperature.

[18] THEMIS surface spectra (average of 50 × 50 pixels) were extracted from the wall ring, the northeastern wall, and the eastern wall from images I34488006, I34800002, and I35137002 (Figure 6). The spectra all show a relatively deep absorption in band 4 (8.56 μm) and band 5 (9.35 μm) consistent with sulfates, high silica phases, or a mixture of the two [*Baldridge and Christensen*, 2006; *Bandfield*, 2008; *McDowell and Hamilton*, 2009]. Phyllosilicates and high silica phases have absorptions near THEMIS band 5, whereas

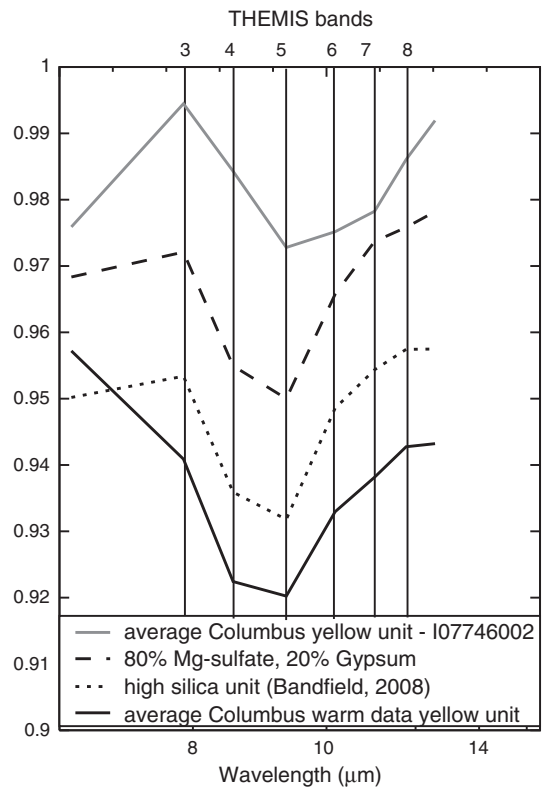

Figure 6. Average THEMIS surface emissivity spectra from yellow surfaces exposed in I34488006, I34800002, and I35137002 (bottom; black). This spectrum resembles the high silica unit identified by *Bandfield* [2006] (dotted) but can also be modeled by a linear combination of Mg and Ca sulfate (dashed). The top (gray) spectrum is the average THEMIS surface emissivity spectra from I07746002. Comparison of the old (top) spectrum with the new (bottom) spectrum shows that the new warmer data are much more consistent with the presence of sulfates.

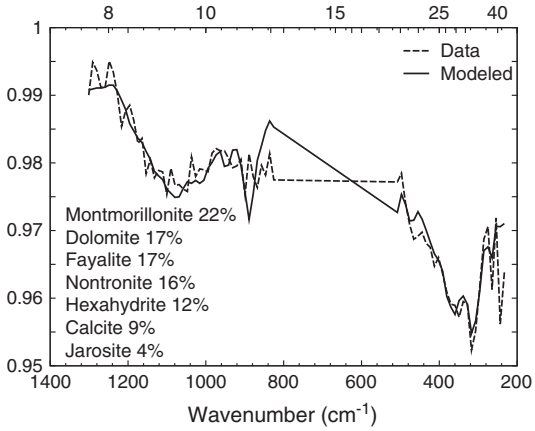

Figure 7. Average TES surface emissivity of the yellow unit at the base of the northeast wall as seen in I34488006. Spectral unmixing with a standard library of end-members indicates high concentrations of clays, olivine, and sulfates.

sulfates tend to have slightly shorter wavelength absorptions nearer to THEMIS band 4. Because both types of materials have strong absorptions between bands 4 and 5, in a 9-6-4 DCS image, both materials appear yellow (high in the red and green bands and low in the blue band) and are difficult to distinguish in THEMIS resolution spectra. However, in the DCS images, phyllosilicates may appear slightly more yellow/green (slightly higher in blue; in this case, band 4), whereas sulfates may appear slightly more yellow/orange (slightly higher in red; in this case, band 9). The wall ring, although it does not appear yellow in the DCS image (see Discussion), has a spectral character similar to the other two yellow units. Compared with the average spectrum extracted from I07746002, the spectra from the newer images are much more consistent with sulfate minerals and are can be modeled by a mixture of Ca and Mg sulfate (Figure 6).

[19] Unmixing results for the average TES spectrum over the unit at the base of the northeast wall is interpreted to represent the highest percentage of clay minerals, olivine, and sulfates (Figure 7). The olivine is likely related to the ejecta in the central portion of the crater, and the presence of phyllosilicates and sulfates is consistent with CRISM detections [*Wray et al*., 2011].

[20] Concentration maps of the crater suggest that concentrations of the sulfate/phyllosilicate end-member occur at the base of the eastern wall and generally correspond to this exposed wall-base unit and the crater wall. However, as would be expected from CRISM results, THEMIS concentrations of the sulfate/phyllosilicate end-member do not appear to correspond with the wall-ring unit (Figure 8). The occurrence of the regional TES surface end-member is concentrated on the crater floor and not in the crater walls nor in the wall-base unit.

5. Discussion

[21] The newer THEMIS (warmer surface) data appear to have a greater potential to identify the presence of low

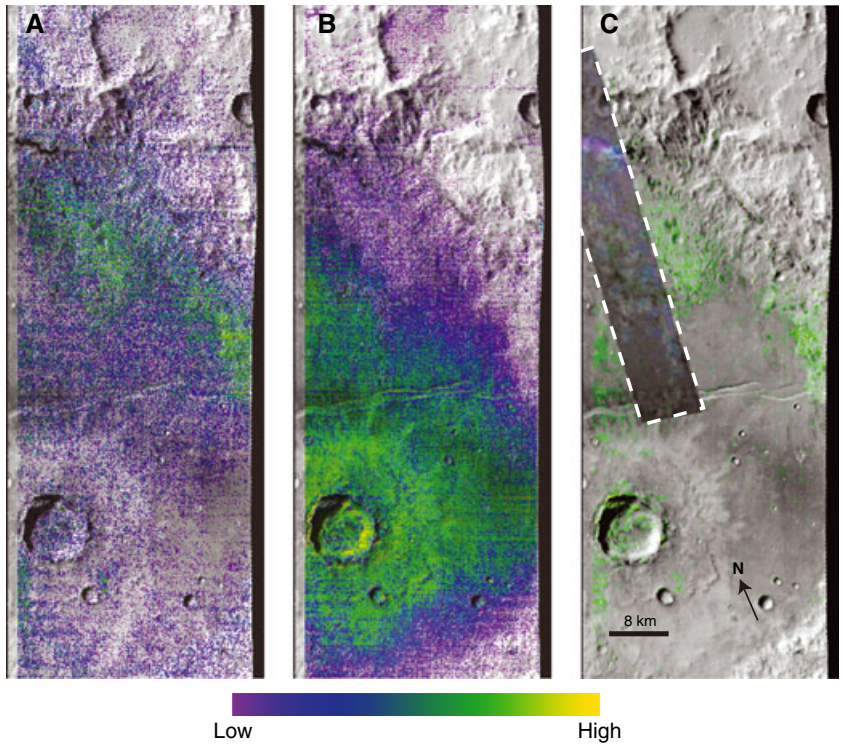

Figure 8. Spectral unit concentration maps for TES regional surface (A) and sulfate/phyllosilicate end-members [*Bandfield et al*., 2004] (B) for THEMIS image I34488006. Colors are draped over grayscale band 9 radiance images for context. Purple represents relatively low concentration, and yellow is relatively high concentration. (C) For comparison, CRISM detections of sulfates using are overlain in blue within the white dashed box (modified from *Wray et al*. [2011]) overlain on THEMIS sulfate/high silica detections (green).

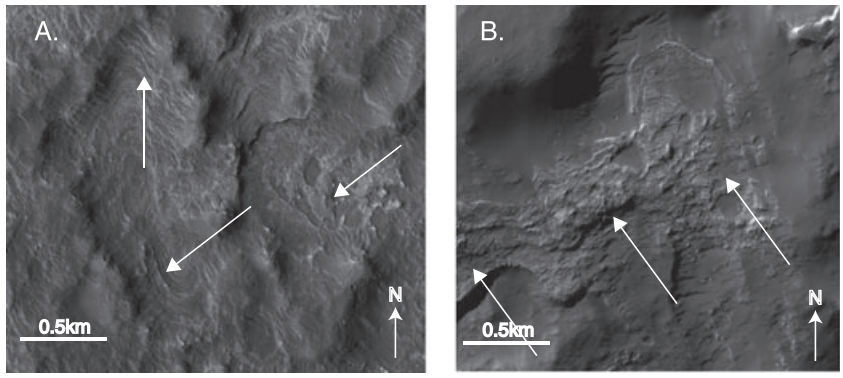

Figure 9. HiRISE images PSP_003306_1510_RED (A) and PSP_003306_1510_RED (B) demonstrate the differences in the wall-base unit and the wall-ring unit, respectively. The wall-base unit contains eroded meter-scale sedimentary layers that show some evidence of cementation. The wall-ring unit is consistent with a more rocky or indurated material that is eroding to mantle the lower crater wall and floor.

spectral contrast minerals such as sulfates and clays than the data from earlier orbits (colder surface) allowed. Based on the SNR/noise equivalent spectral radiance values reported by *Christensen et al*. [2004] in the THEMIS calibration report, it is possible to estimate the SNR of the newly acquired warm data. We estimate the SNR for data with surface temperatures of 295 K to be approximately 260 compared with the SNR of 179 for cooler 270 K data and the SNR of 115 for data with a surface temperature of 245 K. This increase in SNR is dramatic and significantly increases the ability to definitively identify previously challenging mineralogy. However, it should be noted that typically single pixels are not analyzed in THEMIS data and 100 s of pixels are typically coadded with random noise decreasing as $n^{1/2}$, where systematic errors are significantly higher than random noise error.

[22] However, high silica phases and sulfate minerals are difficult to distinguish at the spectral resolution of THEMIS data. These minerals are associated with small outcrops (<1 km thick) and identified in close proximity in the CRISM data [*Wray et al*., 2011]. There these minerals are indistinguishable at the spatial resolution of the TES instrument (~3 km). A narrow absorption present in the TES data at 22 m is characteristic of phyllosilicates [*Michalski et al*., 2006], but the yellow units in the THEMIS concentration maps are better fit with sulfates rather than phyllosilicates. Nonetheless, the presence of both sulfates and phyllosilicates is consistent with the VNIR data [*Wray et al*., 2011]. In the CRISM data, the sulfates and phyllosilicates appear to be interbedded in some places within the crater and would therefore be indistinguishable at THEMIS spectral/spatial resolution. Indeed, on Earth, phyllosilicates and sulfates often occur together or in close proximity in aqueous settings (a suggested environment of deposition for Columbus crater [*Wray et al*., 2011]), so the detection of one may suggest the presence of the other [*Baldridge et al*., 2009].

[23] Even with the newer orbit and warmer data, no spectral evidence can be gleaned from the higher thermal inertia wall-ring unit (Figure 2), although the wall unit contains the highest concentration of sulfate minerals in Columbus crater as indicated by CRISM data [*Wray et al*., 2011]. High-Resolution Imaging Science Experiment (HiRISE) images of the wall ring suggest that it represents an indurated evaporite (Figure 9) [*Wray et al*., 2011], which is supported by higher relative thermal inertia data (158 J K^{-1} m^{-2} $s^{-1/2}$ for the floor compared with 343 J K^{-1} m^{-2} $s^{-1/2}$ for the wall). All of these factors should result in a strong signature in the IR distinct from the ubiquitous basalt spectra. Although

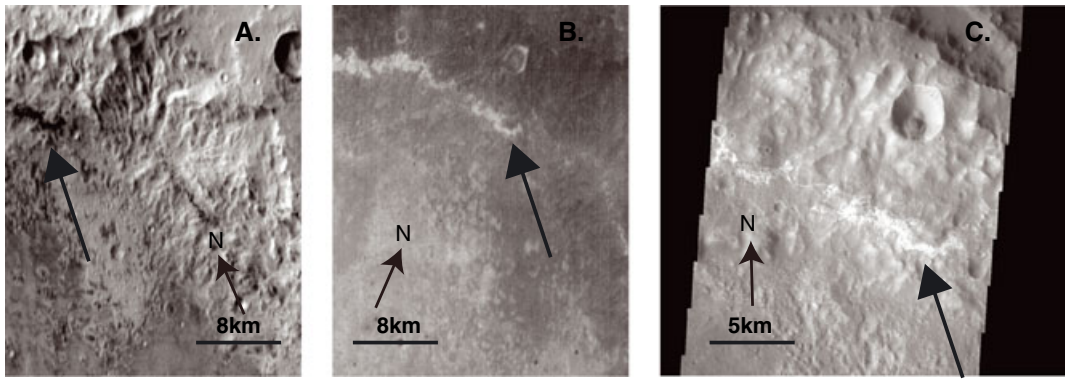

Figure 10. Columbus crater wall ring as seen in THEMIS day IR band 9 (A; I34488006), night IR band 9 (B; I34357007), and visible band 3 (C; V15571005) images. Arrows point to the ring unit. The ring appears bright in the visible images, dark in daytime IR, and bright in nighttime IR. This relationship indicates that the unit has a high thermal inertia and should have a strong emissivity signature.

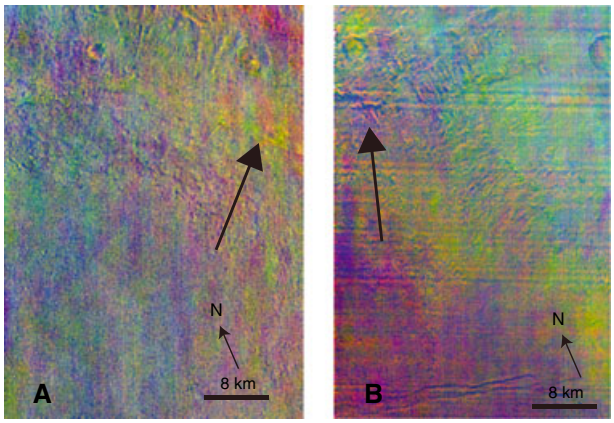

Figure 11. DCS THEMIS emissivity images I07746002 (A) and I34488006 (B). Bands 9, 6, and 4 were projected as red, green, and blue, respectively, as in Figures 4 and 5. In processing an image to emissivity from radiance, all effects of temperature should be removed. In the newer data, the wall ring appears dark, indicating either incomplete temperature removal occurred or that the unit is indistinct from the surrounding material.

the ring appears bright in THEMIS visible, dark in THEMIS daytime IR, and bright in THEMIS nighttime IR (Figure 10), in the more recent, warmer data, the ring does not have a distinct color in any band combination emissivity DCS images (e.g., Figure 5). This is seems odd, because the wall ring has a distinct yellow tone in the warmest of the old later time-of-day DCS images (I07746002; Figure 11). Instead, the wall ring is dark, indicating either incomplete temperature removal or that the unit is indistinct from the surrounding wall. Alternately, in these same images, the floor unit, which has lower-strength absorption features of sulfates and phyllosilicates than in the CRISM data of the wall unit, has a very distinct phyllosilicate or sulfate spectral signature in the THEMIS IR data. Why are the floor deposits much more distinguishable in the earlier time-of-day, warmer THEMIS data? This apparent discrepancy is likely due to differences in the diurnal temperature curve for the two types of units (Figure 1) and their levels of induration/particle size. In the new orbit time (~15:00) of the Mars Odyssey spacecraft, the moderate thermal inertia wall unit remains significantly cooler than the low thermal inertia crater floor (~10–15 K lower) material, which exhibits the spectral character of sulfate-bearing materials in THEMIS data. During the old orbit time (~17:30) of the Mars Odyssey spacecraft, the data show both the high thermal inertia walls unit and the low thermal inertia crater floor unit both have approximately similar (and low) predicted temperatures. The only conditions for which sulfate materials are detected in THEMIS data correspond to the low thermal inertia materials, which achieve higher surface kinetic temperatures and consequently higher SNR but are more difficult to identify specific sulfate mineralogy due to decreased fundamental band contrast. To support this, HiRISE images of the wall-base unit show meter-scale stratification indicative of sedimentary units, whereas images of the wall ring seem more indicative of rock materials that are being exhumed from the wall (Figure 9). The floor unit at the base of the crater wall may represent a highly degraded alluvial fan, which is mantled by fine-grained hydrated material eroded from the crater wall ring [*Wray et al.*, 2011]. The floor has a lower thermal inertia, indicating that it is less indurated than the wall ring. Higher thermal inertia units should have a stronger IR spectral signature than lower thermal inertia units [*Vincent and Hunt*, 1968], because the effects of particle scattering are minimized from a more solid material. However, lower thermal inertia materials achieve higher surface kinetic temperatures in the late afternoon compared with higher thermal inertia material (Figure 12) and consequently higher SNR. In the early afternoon THEMIS data, this allows for the detection of sulfates and phyllosilicates in the lower thermal inertia units but not in the indurated wall unit.

6. Conclusions

[24] Columbus crater has excellent coverage with THEMIS IR data: there is complete coverage both before and after the move to an earlier orbit time. However, aqueous minerals only appear distinct in a few of the images. In these images, earlier time-of-day and proper seasonal observations combine to provide warm surface temperatures that significantly increase the ability to identify low spectral contrast aqueous

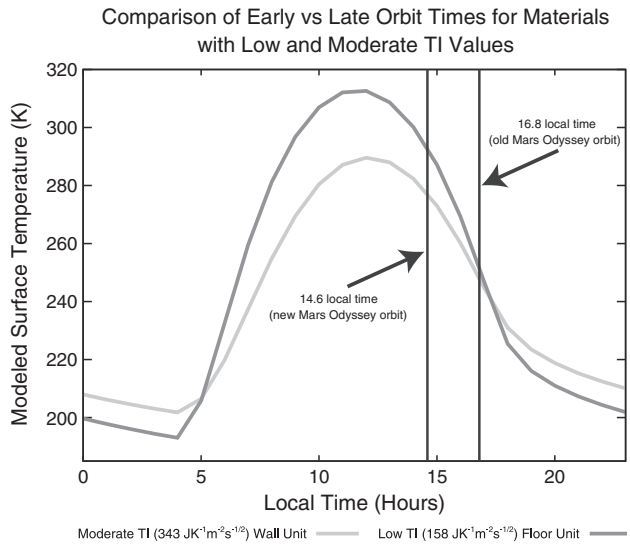

Figure 12. We used the KRC [*Kieffer*, 2012, in press] thermal model to calculate the diurnal surface temperature curves for the materials of two different thermal inertia values observed in Columbus crater [sulfate-bearing moderate thermal inertia wall (343 J K^{-1} m^{-2} $s^{-1/2}$) unit and the sulfate-bearing low thermal inertia floor (158 J K^{-1} m^{-2} $s^{-1/2}$) unit]. In the new orbit time (~15:00) of the Mars Odyssey spacecraft, the moderate thermal inertia wall unit remains significantly cooler than the low thermal inertia crater floor (~10–15 K lower) material, which exhibits the spectral character of sulfate-bearing materials in THEMIS data. During the old orbit time (~17:30) of the Mars Odyssey spacecraft, the data show both the high thermal inertia walls unit and the low thermal inertia crater floor unit both having approximately similar (and low) predicted temperatures.

minerals. The ideal conditions required to detect these low spectral contrast units in THEMIS data are dependent on several factors. The following observations were required for a positive identification of sulfates in Columbus crater based on THEMIS data:

[25] 1. The average surface temperature for the images in which the aqueous deposits are detected is 270 K. This is approximately 20° warmer than most images taken before the orbit change. However, Sun-facing slopes in the warmest images observed (maximum surface temperature >300 K) were saturated so it appears that there is either a limit to the temperatures at which surfaces can be observed or an observation error that needs further study.

[26] 2. Warmer surface temperatures are related to the time of year that images are observed. The THEMIS observations in which the aqueous deposits are detected occur during the late southern summer (Ls ~ 270–360). The southern summer, although ideal in terms of surface temperatures, is also commonly a time of the year for Martian dust storms occur (because Mars lies closest to the Sun and solar heating is greatest). Therefore, ideal observation conditions (i.e., atmospheric dust opacity is low and surface temperatures are high) occur in the late summer after the major dust storm season has ended [*Christensen et al*., 2004].

[27] 3. Diurnal temperature curves for Mars (Figure 12) show the warmest surface temperatures on Mars lag noon by approximately 3 hours, before the surface begins to cool again. Therefore, to optimize the SNR in the data, it is ideal to observe the surface close to approximately 15:00 LMST, before the surface begins to cool.

[28] 4. Beginning with the third extended mission, Odyssey is currently in a 15:45 LMST orbit rather than the 16:15 LMST orbit in the earlier phases of the mission. The 16:15 orbit meant that images were being taken after the surface had cooled significantly (~20°) from the maximum daytime temperature.

[29] Earlier time-of-day and proper seasonal observations combine to provide warm surface temperatures and ideal low atmospheric opacity for the observation of low spectral contrast aqueous minerals at the surface of Mars. It is fortuitous that these conditions occurred over Columbus crater, where several aqueous minerals have been detected in the VNIR spectral range, and that the presence of these minerals could be confirmed by THEMIS. It is unfortunate that these favorable observation conditions did not occur during the first 8 years of the THEMIS experiment, inhibiting one of the primary goals of the experiment: to identify minerals associated with hydrothermal and sub-aqueous environments. The CRISM data have proven to be invaluable in identifying specific aqueous minerals for local regions on Mars. However, THEMIS data coverage is significantly better (100% of the planet in day IR) and early afternoon (warmer) THEMIS data should prove important in identifying larger scales of aqueous mineralogy to support further investigations with higher resolution data. The Odyssey orbit is slowly drifting to later times of day to support future landed missions (e.g., Mars Science Laboratory), but there are several more Martian summers of earlier time-of-day observations in addition to archives of 2009 and 2012 observations and these warmer observations may reveal additional evidence for aqueously formed minerals.

[30] **Acknowledgments.** Aspects of this work were funded through the Mars Data Analysis and Mars Odyssey Participating Scientist Programs. Special thanks to Mikki Osterloo and to an anonymous reviewer for comments that significantly improved the manuscript. The authors would also like to thank Josh Bandfield for support throughout the writing of the manuscript and discussions regarding SNR.

References

Baldridge, A., and P. Christensen (2006), Detection of Sulfates in Meridiani Planum With THEMIS TIR Data, *AGU Fall Meeting Abstracts*, *23*, 0066.

Baldridge, A. M. (2008), Thermal Infrared Spectral Studies of Sulfates and Chlorides; Applications to Salts on the Martian Surface, Ph.D. Dissertation thesis, 204 pp., Arizona State University, Tempe, AZ.

Baldridge, A. M., and P. Christensen (2004), Spectroscopy of Salt-Cemented Materials; Evidence for the Occurrence of Water in the Martian Surface Layer, *AGU Fall Meeting Abstracts*, *21*, 0209.

Baldridge, A. M., S. J. Hook, C. R. Souza Filho, B. J. Thomson, N. T. Bridges, and J. K. Crowley (2009), Exploring Variability in Acidic Saline Playa Lakes in WA with HyMAP Hyperspectral Data, *AGU Fall Meeting Abstracts*, *23*, 1235.

Bandfield, J. L. (2008), High-silica deposits of an aqueous origin in western Hellas Basin, *Mars, GRL*, *35*, 12205.

Bandfield, J. L., P. R. Christensen, and M. D. Smith (2000a), Spectral data set factor analysis and end-member recovery: Application to analysis of Martian atmospheric particulates, *J. Geophys. Res.*, *105*, 9573–9588.

Bandfield, J. L., V. E. Hamilton, and P. R. Christensen (2000b), A Global View of Martian Surface Compositions from MGS-TES, *Science*, *287*, 1626–1630.

Bandfield, J. L., A. Deanne Rogers, and C. S. Edwards (2011), The role of aqueous alteration in the formation of Martian soils, *Icarus*, *211*, 157–171.

Bandfield, J. L., D. Rogers, M. D. Smith, and P. R. Christensen (2004), Atmospheric correction and surface spectral unit mapping using Thermal Emission Imaging System data, *J. Geophys. Res.*, *109*, 10008.

Burns, R. G. (1987), Ferric sulfates on Mars, *J. Geophys. Res.*, *92*, 570.

Christensen, P. R. (2011), edited.

Christensen, P. R., J. L. Bandfield, V. E. Hamilton, D. A. Howard, M. D. Lane, J. L. Piatek, S. W. Ruff, and W. L. Stefanov (2000), A Thermal Emission Spectral Library of Rock-Forming Minerals, *J. Geophys. Res.*, *105*(E4), 9735.

Christensen, P. R., et al. (2004), The Thermal Emission Imaging System (THEMIS) for the Mars 2001 Odyssey Mission, *Space Sci Rev*, *110*(1-2), 85–130.

Christensen, P. R., et al. (2003), Morphology and composition of the surface of Mars: Mars Odyssey THEMIS results, *Science*, *300*(5628), 2056–2061.

Clark, B. C., and D. C. Van Hart (1981), The salts of Mars, *Icarus*, *45*(2), 370–378.

Edwards, C. S., P. R. Christensen, and V. E. Hamilton (2008), Evidence for extensive olivine-rich basalt bedrock outcrops in Ganges and Eos chasmas, Mars, *J. Geophys. Res.*, *113*, 11003.

Edwards, C. S., K. J. Nowicki, P. R. Christensen, J. Hill, N. Gorelick, and K. Murray (2011), Mosaicking of global planetary image datasets: 1. Techniques and data processing for Thermal Emission Imaging System (THEMIS) multi-spectral data, *J. Geophys. Res.*, *116*(E10), E10008.

Farmer, V. C. (1974), *The Infrared Spectra of Minerals*, Mineralogical Society, London.

Gendrin, A., et al. (2005), Sulfates in Martian Layered Terrains: The OMEGA/Mars Express View, *Science*, *307*(5715), 1587.

Gillespie, A. R., A. B. Kahle, and R. E. Walker (1986), Color enhancement of highly correlated images. I. Decorrelation and HSI contrast stretches, *Remote Sens Environ*, *20*(3), 209–235.

Glotch, T. D., J. L. Bandfield, P. R. Christensen, W. M. Calvin, S. M. McLennan, B. C. Clark, A. D. Rogers, and S. W. Squyres (2006), Mineralogy of the Light-Toned Outcrop at Meridiani Planum as seen by the Miniature Thermal Emission Spectrometer and Implications for its Formation, *J. Geophys. Res.*, *111*(E12), E12S03.

Hamilton, V. E., and P. R. Christensen (2005), Evidence for extensive, olivine-rich bedrock on Mars, *Geology*, *33*(6), 433–436.

Kieffer, H. H. (2012), Thermal model for analysis of Mars infrared mapping, *J. Geophys. Res.*, *118*, doi:10.1029/2012JE004164.

Klingelhofer, G., et al. (2004), Jarosite and Hematite at Meridiani Planum from Opportunity's Mossbauer Spectrometer, *Science*, *306*, 1740–1745.

Lane, M. D. (2007), Mid-Infrared Emission Spectroscopy of Sulfate and Sulfate-Bearing Minerals, *Am. Mineral.*, *92*(1), 1.

Lane, M. D., J. L. Bishop, M. D. Dyar, P. L. King, M. Parente, and B. C. Hyde (2008), Mineralogy of the Paso Robles Soil on Mars, *Am. Mineral.*, *93*(5-6), 728–739.

Langevin, Y., F. Poulet, J.-P. Bibring, and B. Gondet (2005), Sulfates in the North Polar Region of Mars Detected by OMEGA/Mars Express, *Science*, *307*, 1584–1586.

Lichtenberg, K. A., et al. (2009), Stratigraphy of hydrated sulfated in the sedimentary deposits of Aram Chaos, *Mars, J. Geophys. Res.*, *115*, E00D17.

McDowell, M. L., and V. E. Hamilton (2009), Seeking phyllosilicates in thermal infrared data: A laboratory and Martian data case study, *J. Geophys. Res.*, *114*(E6), E06007.

Mellon, M. T., B. M. Jakosky, H. H. Kieffer, and P. R. Christensen (2000), High-resolution thermal inertia mapping from the Mars Global Surveyor Thermal Emission Spectrometer, *Icarus*, *148*(2), 437–455.

Michalski, J. R., M. D. Kraft, T. G. Sharp, L. B. Williams, and P. R. Christensen (2006), Emission spectroscopy of clay minerals and evidence for poorly crystalline aluminosilicates on Mars from Thermal Emission Spectrometer data, *J. Geophys. Res.*, *111*(E3), E03004.

Osterloo, M. M., F. S. Anderson, V. E. Hamilton, and T. D. Glotch (2007), Analysis of a Spectrally Distinct Surface Feature in the Terra Sirenum Region of Mars from THEMIS and TES, paper presented at Lunar and Planetary Institute Conference March 1, 2007.

Osterloo, M. M., V. E. Hamilton, F. S. Anderson, and W. C. Koeppen (2009), THEMIS Detections of Forsterite-Fayalite Compositions Within Terra Tyrrhena, in *Lunar and Planetary Institute Science Conference Abstracts*, edited, p. 1405.

Ramsey, M. S., and P. R. Christensen (1998), Mineral abundance determination: Quantitative deconvolution of thermal emission spectra, *J. Geophys. Res.*, *103*(B1), 577–596.

Rogers, A. D., and P. R. Christensen (2007), Surface mineralogy of Martian low-albedo regions from MGS-TES data: Implications for upper crustal evolution and surface alteration, *J. Geophys. Res.*, *112*(E1), E01003.

Rogers, A. D., P. R. Christensen, and J. L. Bandfield (2005), Compositional heterogeneity of the ancient Martian crust: Analysis of Ares Vallis bedrock with THEMIS and TES data, *J. Geophys. Res.*, *110*(E5), E05010.

Rogers, A. D., O. Aharonson, and J. L. Bandfield (2009), Geologic context of in situ rocky exposures in Mare Serpentis, Mars: Implications for crust and regolith evolution in the cratered highlands, *Icarus*, *200*(2), 446–462.

Ruff, S. W., and P. R. Christensen (2002), Bright and Dark Regions on Mars: Particle Size and Mineralogical Characteristics Based on Thermal Emission Spectrometer Data, *J. Geophys. Res.*, *107*(E12), 5127.

Spanovich, N., M. D. Smith, P. H. Smith, M. J. Wolff, P. R. Christensen, and S. W. Squyres (2006), Surface and near-surface atmospheric temperatures for the Mars Exploration Rover landing sites, *Icarus*, *180*(2), 314–320.

Stockstill, K. R., J. E. Moersch, H. Y. McSween, Jr., J. L. Piatek, and P. R. Christensen (2007), TES and THEMIS study of proposed paleolake basins within the Aeolis quadrangle of Mars, *J. Geophys. Res.*, *112*(E01001), doi:10.1029/2005JE002517.

Swayze, G. A., et al. (2008), Discovery of the Acid-Sulfate Mineral Alunite in Terra Sirenum, Mars, Using MRO CRISM: Possible Evidence for Acid-Saline Lacustrine Deposits?, *AGU Fall Meeting Abstracts*, *44*, 04.

Vincent, R. K., and G. R. Hunt (1968), Infrared Reflectance from Mat Surfaces, *Appl Optics*, *7*(1), 53.

Weiss-Malik, M., N. S. Gorelick, and P. R. Christensen (2005), JMARS: A GIS System for Mars and Other Planets, *AGU Fall Meeting Abstracts*, *21*, 0169.

Wray, J. J., S. L. Murchie, S. W. Squyres, F. P. Seelos, and L. L. Tornabene (2009), Diverse aqueous environments on ancient Mars revealed in the southern highlands, *Geology*, *37*, 1043–1046.

Wray, J. J., et al. (2011), Columbus crater and other possible groundwater-fed paleolakes of Terra Sirenum, Mars, *J. Geophys. Res.*, *116*, 01001.